Bull. Mater. Sci., Vol. 7, No. 1, March 1985, pp. 21–30. © Printed in India.

X-ray diffraction study of cation interdiffusion in mixed UO_2-PuO_2 compacts

RAVI VERMA and P R ROY

Radiometallurgy Division, Bhabha Atomic Research Centre, Bombay 400 085, India

Abstract. Cation interdiffusion kinetics in mixed oxide ($UO_2 + PuO_2$) compacts is studied using x-ray powder diffraction technique. A profile deconvolution method based on Fourier analysis is developed and used to characterise the degree of homogenisation in the sintered compacts. A concentric core-shell diffusion model in which UO_2 constitutes a solute core enveloped by PuO_2, acting as solvent, is adopted. The radial diffusion equation is solved for appropriate boundary conditions to yield a relationship between the annealing time and the degree of homogenisation. This relationship is used to estimate the interdiffusion coefficients at various temperatures.

Keywords. Homogenisation; cation interdiffusion; UO_2-PuO_2; powder compacts; x-ray diffraction.

1. Introduction

In the production of (U, Pu)O_2 fuel for nuclear reactors, a knowledge of cation interdiffusion in UO_2-PuO_2 system is required to predict metal atom homogenisation during the sintering of the fuel compacts. Although a large amount of cation diffusion data is reported (Marin and Contamin 1968; Matzke 1968; Belle 1969), there is no general agreement amongst the various sets of data. The reasons for this disagreement are: experimental limitations of the methods employed, contribution of grain boundary diffusion to the measured diffusion coefficients (Alcock *et al* 1966; Theisen and Vollath 1967) and the effect of impurities and non-stoichiometry on the cation diffusivity (Lidiard 1966; Matzke 1966). It is realised that one needs to generate ones own data typical of the conditions of fuel production and the state of the starting UO_2 and PuO_2 powders.

This paper presents an x-ray line profile analysis method of quantifying inhomogeneity in sintered UO_2-PuO_2 compacts. The method is used to study cation interdiffusion kinetics in these compacts.

2. Experimental

Characteristics of the UO_2 and the PuO_2 powders used are given in table 1. The two powders were mixed in equal proportions by weight, blended for 2 hr in a planetary ball mill, granulated and compacted into pellets at 150 MPa. The pellets were sintered at 1573, 1673, 1773, 1823 and 1873K, for various time durations in an atomsphere of Ar-8 % H_2. Prior to recording x-ray diffraction patterns, the O/M ratios of the sintered pellets were adjusted to 2·00 by equilibrating the pellets in a suitable oxygen potential (McNeilly and Chickalla 1971). This was done to eliminate x-ray lines broadening due

Table 1. Characteristics of starting powders.

Material	Surface area (m^2/g)	Particle size (μm)	Apparent density (g/cc)	Tap density (g/cc)	Total impurity (ppm)
UO_2	3·0	2·3	1·56	2·59	< 500
PuO_2	13·6	3·2	2·31	3·04	< 2000

to any oxygen inhomogeneity in the sintered pellets (Ravi Verma *et al* 1977). The 311 profiles of all the O/M adjusted pellets were recorded at a scanning speed of 1/8° in 2θ/min using CuKα radiation.

3. Mixed-composition fraction analysis

A sintered UO_2-PuO_2 mixed compact normally comprises a range of mixed compositions between UO_2 and PuO_2. X-ray line profiles recorded from such a material are broadened on account of the above referred inhomogeneity. A broad line profile, infact, can be imagined to consist of a band of closely spaced 'normal' (unbroadened) Bragg lines, one each from the series of mixed compositions present in the compact. Since a Bragg line has a finite instrumental broadening the lines in the band severely overlap each other, and consequently the individual line intensities cannot be read from the experimental line profile. If the experimental profile can be corrected for the instrumental broadening, the x-ray intensities diffracted by different mixed compositions will get confined to delta functions at the respective Bragg angle positions, and the individual intensity contributions of the various mixed compositions will be separately known.

3.1 *Instrumental broadening correction*

A 311 profile obtained from a mixed compact (UO_2-50 % PuO_2) sintered at 1773 K for 2 hr was chosen for the analysis. Stokes method (1948) of profile deconvolution was used to correct the experimental profile for the instrumental broadening. A 311 profile recorded from a well annealed UO_2 compact was chosen to represent the instrumental broadening for this purpose. The intensity values at constant 2θ intervals were measured in both the profiles so as to represent the profiles in terms of about 200 discrete data points. The data were used to compute the Fourier coefficients of the two profiles, from which the Fourier coefficients for the 'pure' diffraction profile were computed. The 'pure' diffraction profile was then synthesized by inverse Fourier transformation. Since only a limited number of terms of the infinite Fourier series could be included in the computation, the profile was computed by terminating the series tentatively at $n = 50$. The detailed analytical procedure is presented elsewhere (Ravi Verma 1983). The synthesized 'pure' diffraction profile showed anomalous oscillations, not related to inhomogeneity. This was inspite of the care taken in the recording of the profile tails and smoothing out the noise in the recorded profile—the recognised sources of errors (Young *et al* 1967; Wilson 1969; Brigham 1974; Delhez and Mittemeijer 1975). It was realised (Ravi Verma 1983) that these oscillations are a result of errors in the higher order Fourier coefficients of the 'pure' diffraction profile, and

that these errors are inherent in the process of computing the Fourier coefficients. These oscillations can be minimized by proper optimization of the termination of the Fourier series. In the present analysis, truncation of series at the harmonic number $n = 25$ gave an almost oscillation free 'pure' diffraction profile of the mixed oxide.

3.2 *Determination of mixed composition fractions*

In the pure diffraction profile, x-ray intensities from different mixed compositions are confined to their respective Bragg angle positions only. An element of area between the ordinates at 2θ and $2\theta + \Delta(2\theta)$ gives the intensity diffracted by only that mixed composition fraction whose Bragg angle is 2θ. Thus, the intensity contributions of various mixed composition fractions are distinctly known.

The x-ray intensity diffracted by a mixed composition depends on its crystal structure factor and volume fraction in the sample. In the system under study, the crystal structure factor can be regarded as constant for all the mixed compositions as the components UO_2 and PuO_2 and the series of solid solutions they form, have the same CaF_2 type crystal structure. Moreover there is very little difference in their lattice parameters ($a_{UO_2} = 5{\cdot}470$ Å, $a_{PUO_2} = 5{\cdot}396$ Å) (Mulford and Ellinger 1958) and the x-ray scattering factors of U and Pu atoms are nearly equal (International tables for x-ray crystallography 1974). Thus in the present case the x-ray intensity diffracted by a particular mixed composition is simply proportional to its volume fraction in the sample.

Now, if the 2θ scale of the 'pure' diffraction profile is changed to a crystal composition scale and the profile is normalised such that its area equals unity (unit volume), the profile will represent the mixed-composition fraction distribution of the mixed oxide sample.

Using Vegards' law (which is obeyed by UO_2-PuO_2 system if the stoichiometry is maintained) (Mulford and Ellinger 1958) and Bragg equation for cubic structure, it can be shown that the composition C (expressed in mole fraction PuO_2) of the mixed oxide is given by

$$C = \frac{1}{a_{UO_2} - a_{PuO_2}} \left(a_{UO_2} - \frac{\lambda\sqrt{S}}{2 \sin\theta} \right) \tag{1}$$

where the symbols have the usual meaning. Equation (1) can be used to change the 2θ scale of the profile to a PuO_2 concentration scale. However, since the possibility of a constant error (shift) in the 2θ scale of the diffractometer trace is not ruled out, only a differential relationship

$$\Delta C = \frac{\lambda\sqrt{S}}{4(a_{UO_2} - a_{PuO_2})} \frac{\cos\theta}{\sin\theta} \Delta(2\theta) \tag{2}$$

is relied upon. In order to draw an absolute PuO_2 concentration scale, the PuO_2 concentration must be known at least at one point on the scale. Use is made of the fact that weighted average PuO_2 concentration of all the mixed compositions in the sample must coincide with the overall PuO_2 concentration in the sample, *i.e.* 50 % PuO_2. With this known concentration at the profile CG as reference an absolute PuO_2 concentration scale was drawn, using (2). The profile was normalised such that the area under the profile was unity. Figure 1 shows the normalised 'pure' diffraction profile which represents the mixed composition fraction distribution of the mixed oxide.

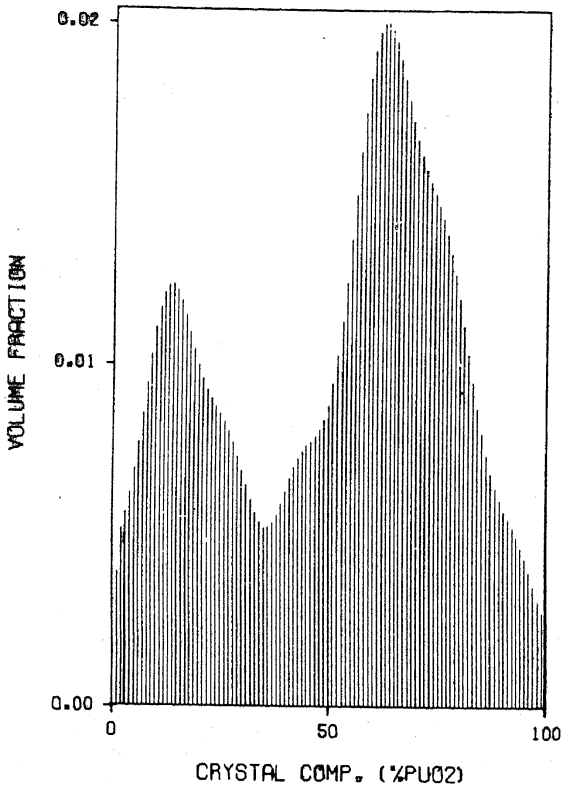

Figure 1. Mixed crystal fraction distribution in (UO_2-50% PuO_2) compact sintered at 1773 K for 2 hr.

4. Homogenisation

4.1 *Observations and phenomenology*

The progress of homogenisation in mixed compacts is followed by observing the merger of x-ray diffraction line profiles of the component phases. In figure (2), 311 profiles of some selected mixed oxide samples are shown. To begin with, two distinct peaks (figure 2a) corresponding to nearly pure UO_2 and PuO_2 phases are observed. As the temperature and/or time of sintering are increased, the PuO_2 based peak progressively increases in intensity and moves towards the UO_2 peak, while the latter decreases in intensity and remains nearly stationary. The process continues till the PuO_2 based peak acquires an intensity equal to the sum of the intensities of pure UO_2 and pure PuO_2 peaks, and the UO_2 peak vanishes (figure 2f). This final peak shows a well resolved $K\alpha_1$-$K\alpha_2$ doublet indicating that the homogenisation is practically complete (Ravi Verma *et al* 1977). This final peak is positioned mid-way between the pure UO_2 and the pure PuO_2 peak positions, implying thereby that the solid solution has acquired the nominal composition $(U_{0.5}Pu_{0.5})O_2$.

It follows from the above observations that the homogenisation in mixed compacts mainly proceeds by the assimilation of UO_2 into the bulk of PuO_2. As a consequence, PuO_2 loses its purity very rapidly, while the undissolved UO_2 at any instant is nearly pure. The process of homogenisation reaches completion when the UO_2 is fully consumed and the PuO_2 based solid solution acquires the average pellet composition.

4.2 *Quantification*

The 311 reflection profiles of all the samples were analysed for mixed-crystal-fractions by the method described in §3. The mixed crystal fraction distributions of some

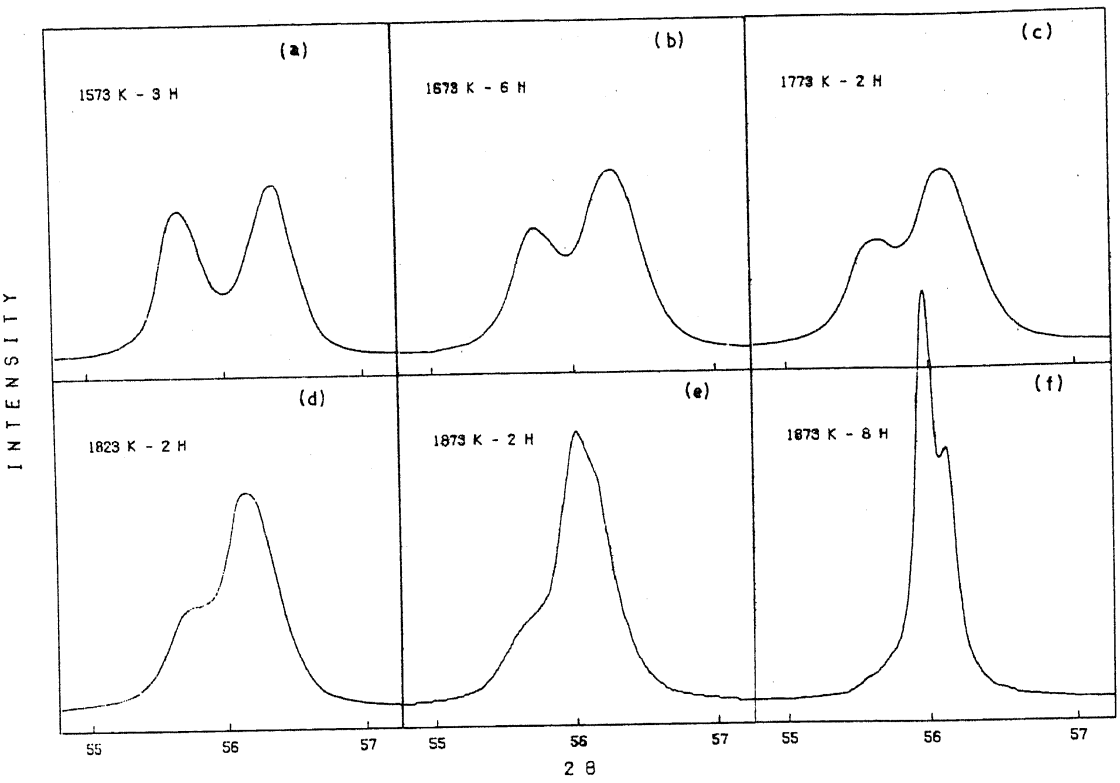

Figure 2. 311 reflection profiles of some sintered mixed UO_2-PuO_2 compacts.

selected samples are shown in figure 3. The anomalous oscillations observed in the mixed crystal fraction distribution corresponding to 1873 K-8 hr are typical of a profile obtained by summation of truncated Fourier series. The amplitude of oscillations is high in case of sharp distribution function. The oscillations have no significance in terms of the sample inhomogeneity.

The observations made in the preceding section suggest that homogenisation attained in the UO_2-PuO_2 mixed compact can be conveniently expressed in terms of the amount of UO_2 that has been assimilated in PuO_2. A complimentary quantity, the amount of UO_2 that remains to be assimilated can be obtained from the mixed crystal distributions of the compacts (figure 3) simply by measuring the area on the UO_2 side of the vertical line through the shallowest point between the two maxima in the distribution. This quantity is plotted against sintering time for different sintering temperatures in figure 4. A corresponding homogenisation scale is also drawn in the figure. The plots show an exponential decrease in the amount of UO_2 with increasing time of sintering at a given sintering temperature. The plots have been redrawn in figure 5 with a logarithmic scale replacing the linear UO_2 scale. The data points lie more or less along straight lines.

5. Interdiffusion model

Homogenisation in mixed UO_2-PuO_2 compacts is a consequence of cation interdiffusion between UO_2 and PuO_2. Based on our observations, it is postulated that the cation flux from UO_2 grain to PuO_2 grain is much larger than that from PuO_2 grain to

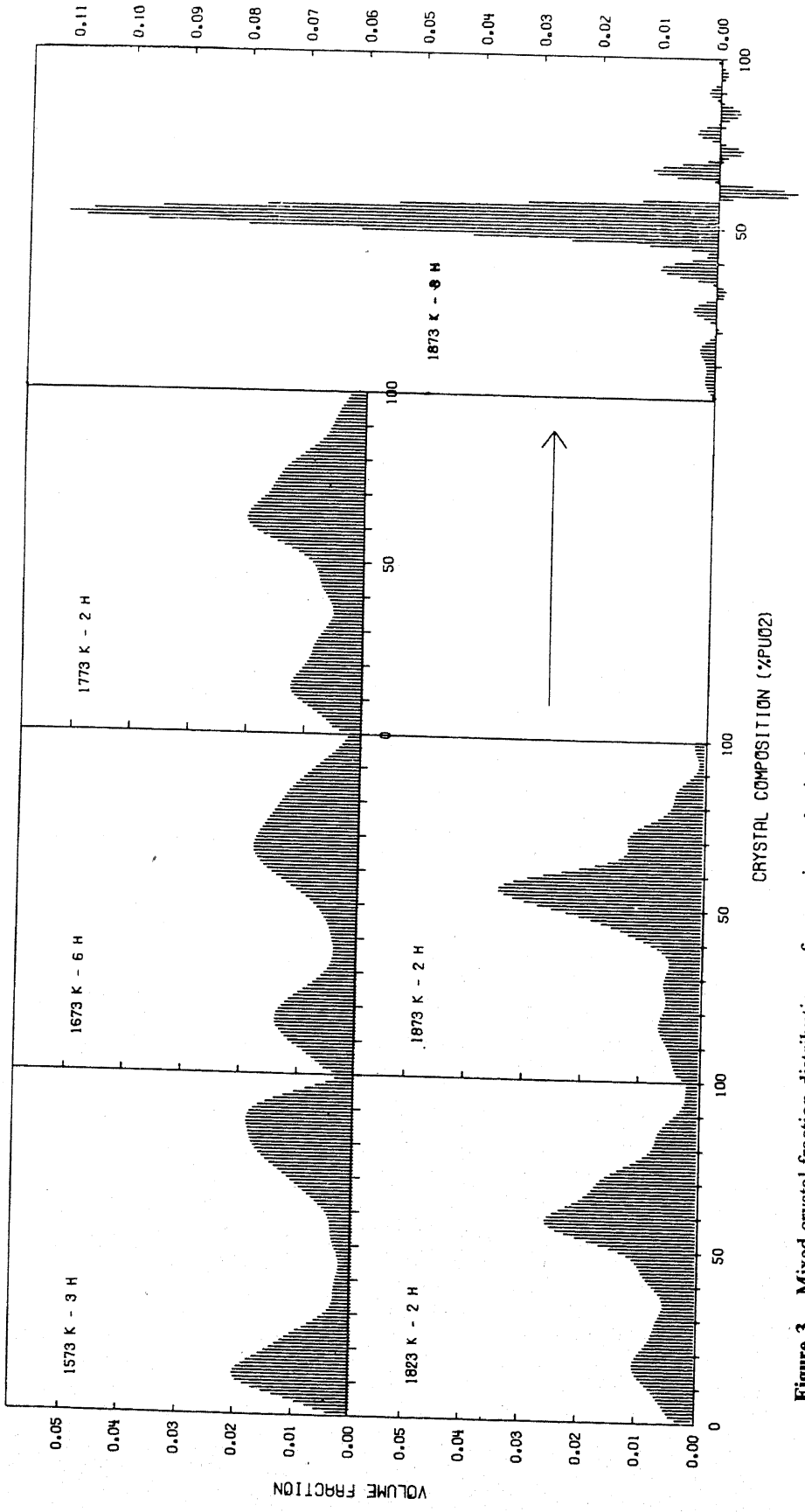

Figure 3. Mixed crystal fraction distributions of some sintered mixed compacts.

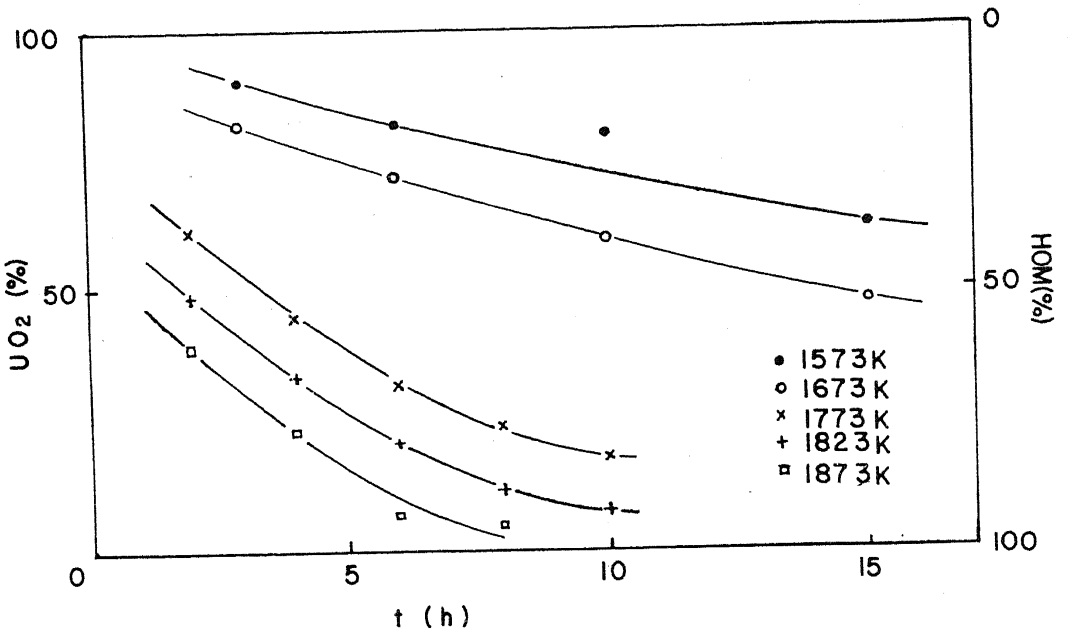

Figure 4. Amount of undissolved UO_2 as a function of time at different annealing temperatures.

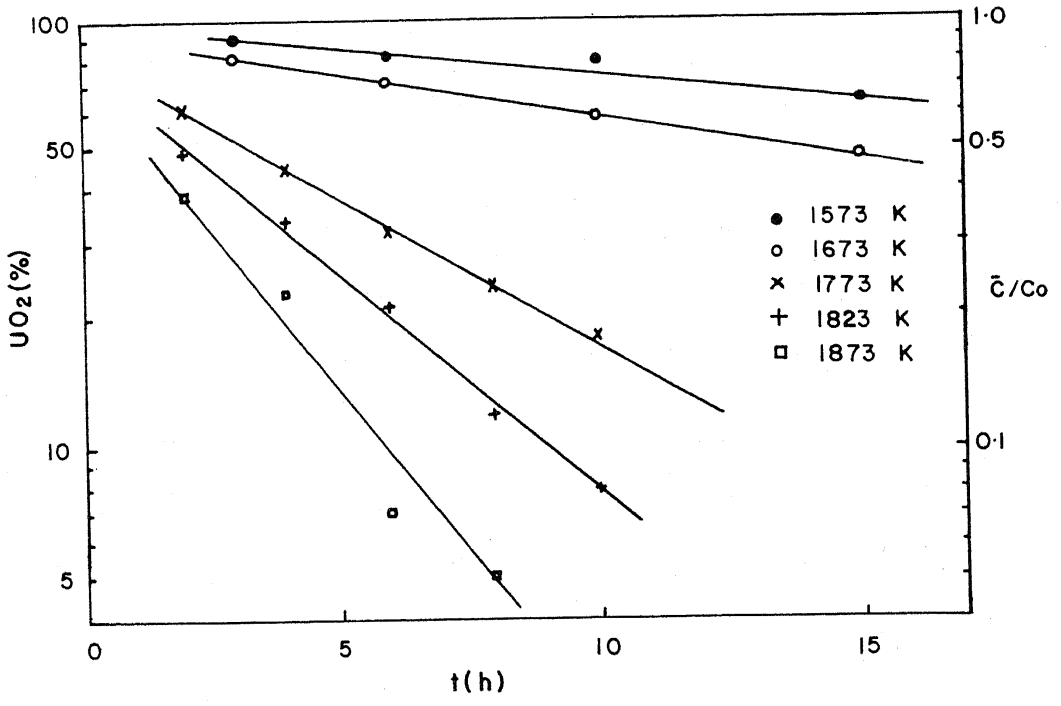

Figure 5. Amount of undissolved UO_2 (log scale) as a function of time at different annealing temperatures.

UO_2 grain, and this gives rise to a net transport of atoms from UO_2 to PuO_2. The PuO_2 grains grow at the cost of the UO_2 grains, pushing the UO_2 grain boundaries inwards akin to Kirkendall effect. Eventually the diminishing UO_2 grains are surrounded by a matrix of PuO_2 based solid solution. Bataller *et al* (1967), in fact, observed islands of UO_2 in a homogeneous (U, Pu)O_2 matrix. Theisen and Vollath (1967) observed that prior to appreciable homogenisation of the mixed compact, PuO_2 envelops UO_2 grains.

The above diffusion configuration was idealised to a concentric core-shell model in which a solute (UO_2) core is surrounded by a solvent (PuO_2) shell. A radial diffusion equation was solved on the lines of Barrer's (1951) solution for diffusion out of a sphere of constant radius containing solute at uniform initial concentration (Ravi Verma 1979). The following equation was derived:

$$D = \frac{a^2}{\pi^2 t} \ln\left(\frac{1{\cdot}16}{\bar{C}/C_0}\right) \tag{3}$$

where D is the chemical diffusion coefficient, a the average UO_2 particle radius, t the time of annealing of the mixed compact and $\bar{C}/C_0$ the fraction of UO_2 remaining undissolved.

6. Results and discussion

To calculate D from (3), the time required to obtain a specified level of homogenisation should be known. The time durations required at different annealing temperatures to attain a dissolution of 90% UO_2 into PuO_2 *i.e.* 10% of UO_2 remaining undissolved ($\bar{C}/C_0 = 0{\cdot}1$) were obtained from the plots in figure 5. The data were used in (3) to calculate the diffusion coefficients. The Arrhenius dependence of diffusivity on temperature is plotted in figure 6. The data points, excepting one, fall on a straight line. The slope of the line gives an activation energy for cation interdiffusion of 222 kJ/mol. The temperature dependence of diffusivity is given by

$$D = 2{\cdot}55 \times 10^{-11} \exp(-2{\cdot}22 \times 10^5/8{\cdot}31\,T)\ \mathrm{m^2/sec}.$$

The diffusivity data obtained above along with the various data on cation diffusion in UO_2 and (U, Pu)O_2 reported in literature are also plotted in figure 6. Agreement amongst the various sets of data is very poor. The data points belonging to this work lie in the middle of the broad band formed by the scatter in the reported data.

The Arrhenius plot in figure 6 fits all the data points very well, except for the one corresponding to 1673 K. The accuracy of this data point, however, cannot be doubted, since like other data points it has been derived from a straight line plot well fitted through four experimental values (figure 5). It is seen that the plots in figure 5 are not uniformly spaced; there is a large gap between the 1673 and 1773 K plots. It suggests that there is, in fact, a discontinuity in the diffusivity plot at some temperature between 1673 and 1773 K. The apparent discontinuity in the diffusivity plot between 1673 and 1773 K needs closer examination.

7. Conclusions

Kinetics of cation interdiffusion can be studied using x-ray line profile analysis method of determining various mixed composition fractions in sintered mixed compacts.

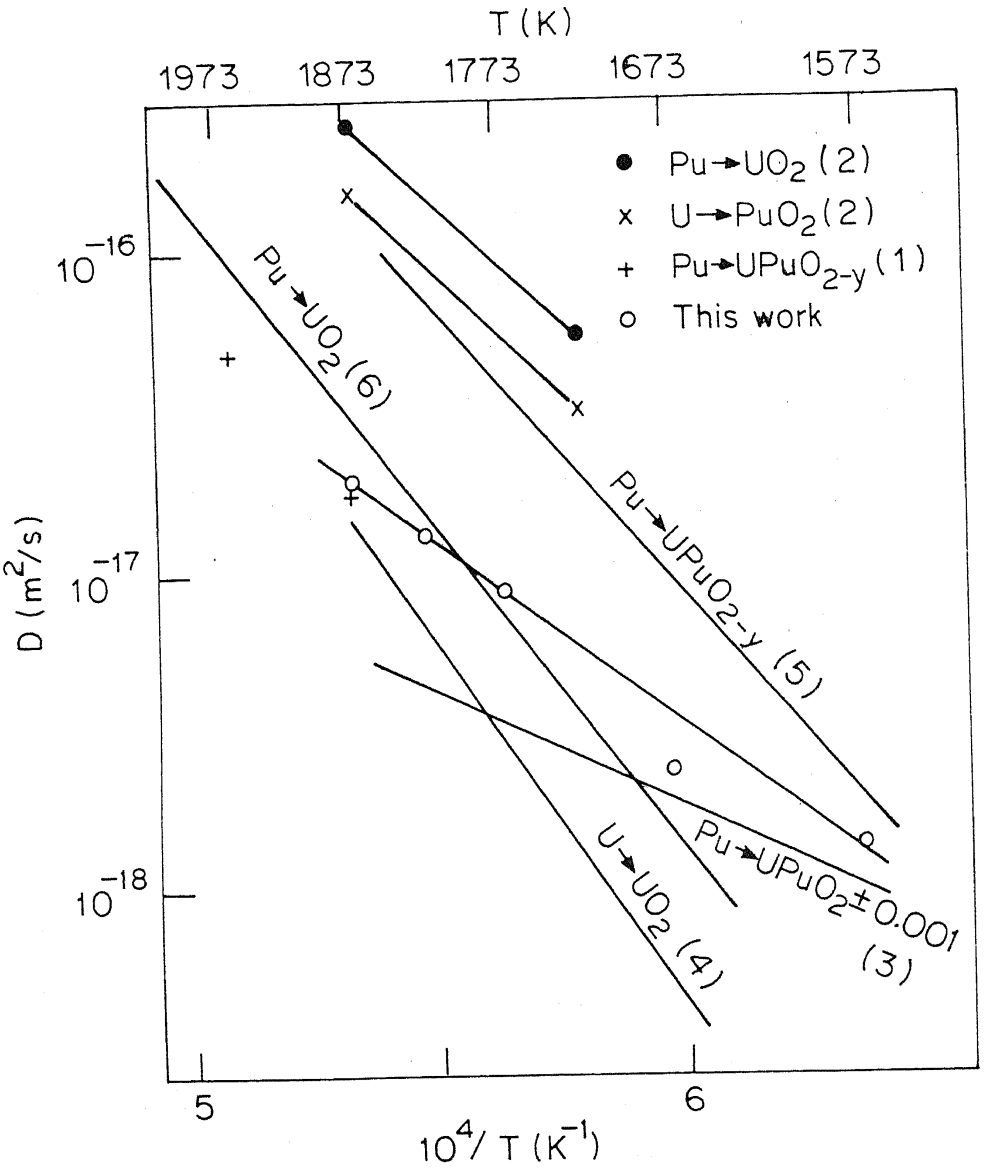

Figure 6. Comparison of various cation diffusion data in UO_2, PuO_2 and $(U, Pu)O_{2\pm x}$: (1) Matzke and Lambert 1973, (2) Theisen and Vollath 1967, (3) Linder *et al* 1967, (4) Linder and Schmitz 1961, (5) Riemer and Scherff 1971 and (6) Schmitz and Linder 1965.

The cation diffusivity in the temperature range studied is given by:

$$D = 2{\cdot}55 \times 10^{-11} \exp(-2{\cdot}22 \times 10^5/8{\cdot}31\,T)\ \mathrm{m}^2/\mathrm{sec}.$$

Acknowledgement

The authors thank Shri S Majumdar and Shri H S Kamath for their co-operation in the experimental part of the work.

References

Alcock C B, Hawkins R J, Hills A W D and McNamara P 1966 in *Thermodynamics* **2** (Vienna: IAEA) p. 57
Barrer R M 1951 *Diffusion in and through solids* (Cambridge: Cambridge University Press) p. 28
Bataller S, Ganivet M, Guillet H, Mosselot Y and Stosskopf F 1967 in *Plutonium as reactor fuel* (Vienna: IAEA) p. 301
Belle J 1969 *J. Nucl. Mater.* **30 3** (and references therein)
Brigham E O 1974 *The fast Fourier transform* (New Jersey: Prentice Hall) p. 91
Delhez R and Mittemeijer E J 1975 *J. Appl. Crystallogr.* **8** 612
International tables for x-ray crystallography 1974 Vol. IV (Birmingham, England: Kynoch Press)
Lidiard A B 1966 *J. Nucl. Mater.* **19** 106
Linder R, Riemann D and Schmitz F 1967 in *Plutonium as reactor fuel* (Vienna: IAEA) p. 265
Linder R and Schmitz F 1961 *Z. Naturforch.* **a16** 1373
Marin J F and Contamin P 1968 *J. Nucl. Mater.* **30** 16 (and references therein)
Matzke Hj 1966 Report AECL 2585 Canada: Chalk River
Matzke Hj 1968 *J. Nucl. Mater.* **30** 26 (and references therein)
Matzke Hj and Lambert R A 1973 *J. Nucl. Mater.* **49** 325
McNeilly C E and Chickalla T D 1971 *J. Nucl. Mater.* **39** 77
Mulford R N R and Ellinger E H 1958 *J. Am. Ceram. Soc.* **80** 2023
Ravi Verma 1979 *J. Nucl. Mater.* **80** 43
Ravi Verma 1983 *J. Nucl. Mater.* **118** 325
Ravi Verma, Mahajan V K and Roy P R 1977 Report BARC/I-433 AEC India
Riemer G and Scherff H L 1971 *J. Nucl. Mater.* **39** 183
Schmitz F and Linder R 1965 *J. Nucl. Mater.* **17** 259
Stokes A R 1948 *Proc. Phys. Soc. Lond.* **61** 382
Theisen R and Vollath D 1967 in *Plutonium as reactor fuel* (Vienna: IAEA) p. 253
Young R A, Gjerdes R J and Wilson A J C 1967 *Acta Crystallogr.* **22** 155
Wilson A J C 1969 *Acta Crystallogr.* **A25** 584